Journal of Environmental Chemical Engineering 4 (2016) 542–548

Contents lists available at ScienceDirect

Journal of Environmental Chemical Engineering

journal homepage: www.elsevier.com/locate/jece

Ilmenite ($FeTiO_3$) as low cost catalyst for advanced oxidation processes

P. García-Muñoz[a,*], G. Pliego[a], J.A. Zazo[a], A. Bahamonde[b], J.A. Casas[a]

[a] Sección departamental de Ingeniería Química, Facultad de Ciencias, Universidad Autónoma de Madrid, 28049 Madrid, Spain
[b] Instituto de Catálisis y Petroleoquímica (CSIC), C/Marie Curie, 2, 28049 Madrid, Spain

ARTICLE INFO

Article history:
Received 3 July 2015
Received in revised form 10 November 2015
Accepted 26 November 2015
Available online 3 December 2015

Keywords:
Ilmenite
CWPO
Photoassisted processes
Solar light
Phenol

ABSTRACT

The role of ilmenite mineral ($FeTiO_3$) in different AOPs processes (photocatalysis, catalytic wet peroxide oxidation (CWPO) and CWPO-Photoassisted processes) was evaluated using phenol as target compound. Our results endorse its role as solar photoassisted catalyst for H_2O_2 decomposing into $HO^{\bullet}$ radicals. In photocatalytic process, despite both the higher TiO_2 content and a band-gap lower than titanium dioxide P25, ilmenite showed a scarce activity. On the other hand, ilmenite results a feasible catalyst in CWPO process, although it requires high induction periods, around 200 min. This drawback can be overcome by combining CWPO with solar light irradiation, since the latest provokes a faster Fe(III) reduction into Fe(II) that decomposes H_2O_2 into $HO^{\bullet}$ radicals. Working at $pH_0 = 3$, $T_0 = 25\,^{\circ}C$, an almost complete phenol ($100\,mg\,L^{-1}$) mineralization ($X_{TOC} > 95\%$) was obtained after 480 min reaction time using the stoichiometric H_2O_2 dose ($500\,mg\,L^{-1}$), ilmenite ($450\,mg\,L^{-1}$) and $550\,W\,m^{-2}$. Besides, Ilmenite showed a high stability after five consecutives CWPO-Photoassisted runs, where TOC reduction, above 90%, was maintained working at the previous experimental conditions. The total Fe leaching from ilmenite was around 2% of the initial load.

1. Introduction

Ilmenite mineral ($FeTiO_3$) have been traditionally used as a raw material for production of TiO_2. Other applications include solar cells, gas sensors and catalysts [1,2].

Since ilmenite contains high percentages of iron and titanium in its structure, it is starting to be employed as heterogeneous catalyst in Advanced Oxidation Processes (AOPs) for the removal of pollutants in wastewater [3].

AOPs represents an interesting alternative to treat wastewater containing pollutants which cannot be eliminated by conventional treatments. These processes generate oxidizing species (especially hydroxyl radical, $HO^{\bullet}$) which oxidize organic chemical compounds [4].

Research on the degradation of hazardous chemical compounds in water by ilmenite as catalyst have been studied upon two different AOPs: as photocatalyst and as catalyst for Catalytic Wet Peroxide Oxidation (CWPO).

Photocatalysis is based on producing hydroxyl radical through irradiating an aqueous TiO_2 suspension with light of $\lambda < 385$ nm for generate valence band holes (h_{VB}^{+}) and conduction band electrons (e^{-}_{CB}) which can migrate to the interface reacting with suitable adsorbed redox species to generate oxidizing species [4].

The results obtained by Moctezuma el al. [5] showed a scarce activity of a synthesized $FeTiO_3$ for phenol photodegradation. On the other hand, ilmenite has demonstrated ability in CWPO process to decompose H_2O_2 due to its iron percentage at acid pH through the redox catalytic cycle of iron combined with H_2O_2 (reaction 1–2) [6].

$$Fe(II) + H_2O_2 \rightarrow Fe(III) + OH^{-} + HO^{\bullet} \quad (1)$$

$$Fe(III) + H_2O_2 \rightarrow Fe(II) + H^{+} + HOO^{\bullet} \quad (2)$$

Teel et al. compared the rates of H_2O_2 decomposition mediated by several minerals at pH 3 to promote the generation of $HO^{\bullet}$ radicals [6]. Despite the high percentage of iron in ilmenite (around 40% in weight), the H_2O_2 decomposition rate was very slow compared to that obtained with the catalysts commonly used in this process, where iron (around 5% in weight) is supported on different materials like carbon, alumina, silica or zeolites. This would indicate that H_2O_2 decomposition occurs mainly on the surface of the catalyst. Nonetheless, the presence of iron in the mineral matrix that acts as active phase in CWPO could lead to a more stable catalyst [7]. Therefore, the feasibility of ilmenite as a

* Corresponding author at: Ingeniería Química, Facultad de Ciencias, C/Francisco Tomás y Valiente 7, Universidad Autónoma de Madrid, 28049 Madrid, Spain.
E-mail addresses: patricia.garciam@uam.es, pgmunoz89@gmail.com (P. García-Muñoz).

http://dx.doi.org/10.1016/j.jece.2015.11.037
2213-3437/

catalyst in these processes require new research to increase the efficiency. In this sense, the activity of iron-containing catalyst can be greatly enhanced by irradiation with light. The reasons of this positive effect on the degradation rate include the photoreduction of Fe(III) to Fe(II) (reaction 3) which produce new $HO^{\bullet}$ radicals with H_2O [8].

$$Fe(III) + H_2O \xrightarrow{h\upsilon} Fe(II) + HO^{\bullet} + H^{+}$$

Therefore, this work aims to study the feasibility of using ilmenite mineral as a catalyst for CWPO process and the synergies of irradiating with solar light. Phenol will be used as target compound since it is a representative industrial wastewater pollutant widely used in AOPs studies and will allow comparing the results obtained with previous iron-supported catalysts.

2. Materials and methods

2.1. Sample characterization

The porous structure of the fresh catalysts was characterized by means of nitrogen adsorption–desorption isotherms at −196 °C using a Micromeritics Tristar 3020 apparatus. The samples were previously outgassed overnight at 150 °C to a residual pressure of 10^{-3} Torr. The iron and titanium content of ilmenite was determined by total reflection X-ray fluorescence (TXRF), using a TXRF spectrometer 8030c. The crystalline phases in the catalyst were analyzed by X-ray diffraction (XRD) using a Siemens model D-5000 diffractometer with Cu Kα radiation. SEM micrographs were obtained in a Hitachi S-3000N apparatus. This equipment was coupled with an energy dispersion X-ray analyser (EDX). Band-gap determination (to estimate the electronic properties) was carried out plotting $(\alpha h\upsilon)^{1/n}$ versus $h\upsilon - E_g \pm E(\Omega)$ (where $n = 2$ for indirect semiconductors) giving a linear absorption edge and its cut with base line corresponds to band-gap energy. The diffuse reflectance spectra were recorded with a UV–vis AgilentVarian, Cary 5000. Ilmenite was also characterized by X-ray Photoelectron Spectroscopy (XPS) using a K-Alpha–Thermo Scientific equipped with a AlKa X-ray excitation source, (1486.68 eV).

2.2. CWPO-Photoassisted runs

The experiments were carried out in an artificial weathering in fast-action instrument Suntest XLS+ (Atlas Material Testing Technology BV, Gelnhausen, Germany) coupled with a Xenon arc lamp of 1700 W adjustable power. The equipment has a Solar ID 65 filter to limit the UV radiation at 320 nm, simulating solar exposition according to ICH Q1B guidelines. The runs were performed adjusting the lamp power to 550 W m^{-2} with a simulated solar emission within 300–800 nm, which corresponds to an average solar radiation in a summer day in southern Europe. The irradiance corresponding to UV radiation was 30 W m^{-2}. The reaction volume was 500 mL and the starting concentration of phenol 100 mg L^{-1}. The catalyst load was 450 mg L^{-1} (preliminary studies showed that the photocatalytic system had an optimal charge of ilmenite of 450 mg L^{-1} because higher and lesser amounts not increase the reaction rate) and the H_2O_2 concentration was 100% of the stoichiometric amount needed for complete mineralization, which is 500 mg L^{-1}. The temperature in the reactor was maintained in the vicinity of 25 °C along all experiments.

2.3. Analytical methods

Phenol and aromatic oxidation by-products were quantified by means of HPLC (Varian Pro-Star 240) using a diode array detector (330 PDA). A Microsorb C18 5 μm column (MV 100, 15 cm long, 4.6 mm diameter) was used as stationary phase and 1 mL min^{-1} of 4 mM aqueous sulfuric solution was used as mobile phase. Short-chain organic acids and chloride ion were analyzed by an ion chromatograph with chemical suppression (Metrohm 790 IC) using a conductivity detector. A Metrosep A supp 5–250 column (25 cm length, 4 mm diameter) was used as the stationary phase, while an aqueous solution containing 3.2 mM Na_2CO_3 and 1 mM $NaHCO_3$ was used as the mobile phase at a flowrate of 0.7 mL min^{-1}. Total organic carbon (TOC) was measured using a TOC analyzer (Shimadzu, model 5000A), while the residual hydrogen peroxide concentration was determined by colorimetric titration using the $TiOSO_4$ method. Leached iron was obtained by ortho-phenanthroline method [9].

3. Results and discussion

3.1. Characterization

The mineral ilmenite ($FeTiO_3$), a Fe/Ti mixed oxide, has a hexagonal structure with two-third of octhaedrical position occupied by cations. Fe and Ti are located in alternative layers. The weight percentage of Fe and Ti in the raw mineral was 36 and 37%, respectively (measured by TXRF). Ilmenite also contains traces of Cr and Mn (0.027% and 1%, respectively). Ilmenite particles were mechanically milled down to $dp < 100$ μm measured with a 100 μm sieve. No further thermal o chemical treatment was applied, in order to address the feasibility of this mineral as received as photocatalyst. The textural analysis from N_2 adsorption-desorption isotherm indicates that ilmenite is a non-porous material with a very low BET Surface, around 6 m^2 g^{-1}.

Fig. 1 shows the results of X-ray Diffraction (XRD) analysis. All diffraction lines were compared to JCPDS card no. 21–1276 and 29–277 due to TiO_2 rutile phase and $FeTiO_3$ phase presence [10]. Intense peaks at $2\theta = 23.9°$, 32.65°, 35.3°, 40°, 48°, 53°, 61°, 63° indicating $FeTiO_3$ in the sample with a crystal size of 6.14 nm. Moreover the peaks at $2\theta = 27°$, 41° and 57° confirming rutile existence. TiO_2 crystals were higher than ilmenite ones which shown a size of 14.9 nm. Phase percentages resulted in 85% $FeTiO_3$ and 15% rutile.

The existence of isolated TiO_2 particles (rutile) and $FeTiO_3$ particles was also confirmed by SEM–EDX images (Fig. 2). On the contrary, no isolated iron oxide particles were found in the mineral.

Additionally, XPS analysis were carried out to determine the Fe (II)/Fe(III) ratio in ilmenite surface [11]. Raghavender et al. defines

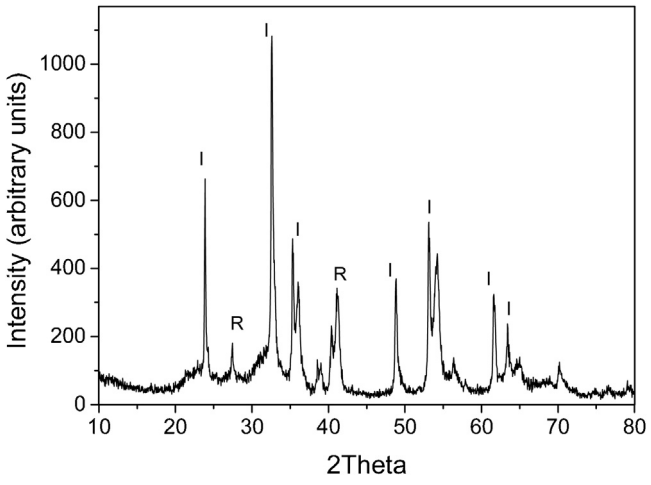

Fig. 1. XRD of ilmenite mineral.

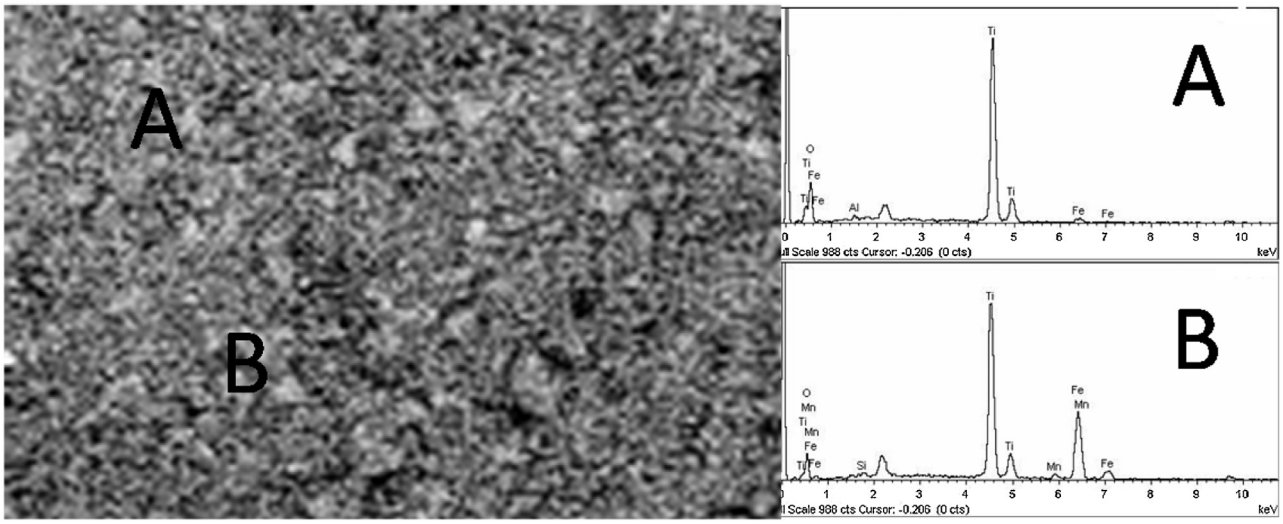

Fig. 2. SEM and EDX of milled ilmenite ($dp < 100\,\mu m$). (A) EDX of TiO_2 particles. (B) EDX of $FeTiO_3$ particles.

ilmenite structure as follows [12]:

$$\left(Fe_x^{2+}, Fe_{1-x}^{3+}\right)_A \left(Ti_x^{4+}, Fe_{1-x}^{3+}\right)_B O_3.$$

Concerning the XPS spectrum of the Fe 2p region (Fig. 3), the presence of a band centered at 710.9 eV can be observed (peak (1)), accompanied by a secondary one 13.2 eV displaced to higher binding energy (724.1 eV)(peak (3)) corresponding to Fe(II). The presence of bands centered in 712.5 and 725.6 eV corresponds to the characteristic values of Fe(III) (peaks (2) and (4)), in addition to a satellite peak around 719.0 eV confirming the presence of Fe^{3+} species in the surface of the studied catalysts (peak 5). The Fe(II)/Fe (III) ratio was 0.56.

The value of the band-gap obtained for ilmenite catalyst was 2.4 eV which means that photocatalytic activity may exist under visible-light irradiation [13]. This value is in agreement with Viswanathan et al. [14], where ilmenite band-gap was between 2.01 and 2.90 eV. It must be noted that this value is lower than the one corresponding to pure titanium dioxide due to the presence of iron which introduces additional electronic states and decrease the band-gap [15].

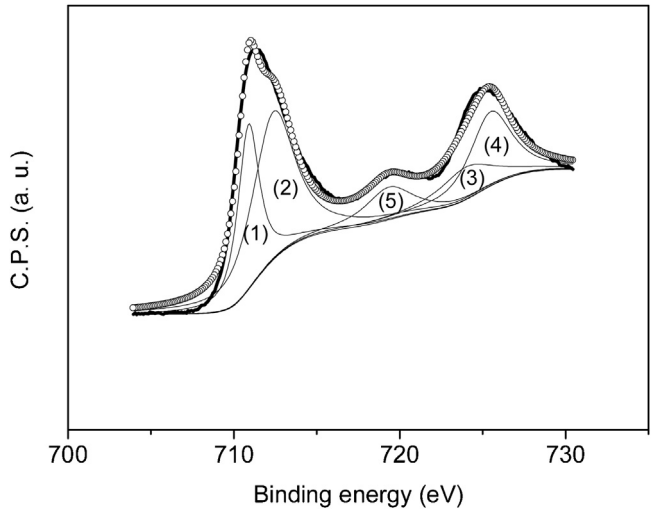

Fig. 3. XPS of Fe 2p region of ilmenite mineral.

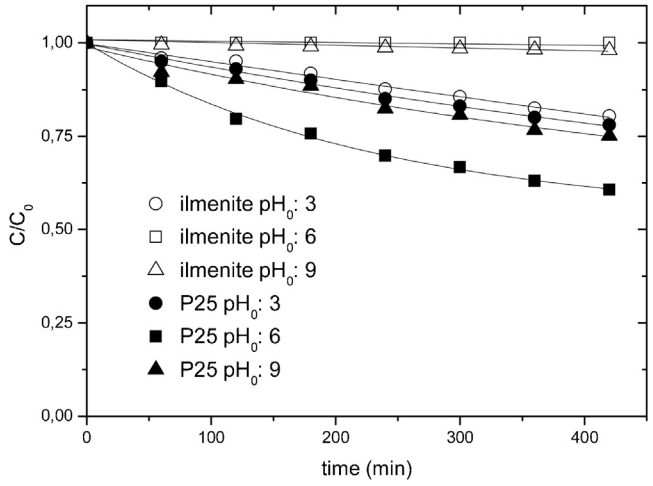

Fig. 4. Evolution of phenol with 450 mg L^{-1} of P25 and ilmenite (operating conditions: [catalyst] = 450 mg L^{-1}; [Phenol] = 100 mg L^{-1}; λ = 300–800 nm; I = 550 W m^{-2}). Lines show trends.

3.3. Photocatalytic activity

Fig. 4 depicts the photocatalytic activity of ilmenite at different initial pHs, in the pH range of 3 to 9 using phenol as model compound. No significant variations in the pH value were observed through the experiments. For the sake of comparison, photocatalytic runs were also carried out with a reference commercial TiO_2 (P25, Evonik-Degussa). Table 1 gathers the rate constants obtained by fitting pseudo first order kinetic model to experimental data. The statistical confidence interval of the kinetic constants are also given.

Table 1
Pseudo-first order rate constants for phenol photodegradation.

Catalyst	pH	$k'_{app} \times 10^3$ (min^{-1})
ILM	3	0.52 ± 0.05
	6	0.01 ± 0.00
	9	0.02 ± 0.00
P25	3	0.60 ± 0.01
	6	1.35 ± 0.02
	9	0.68 ± 0.03

As can be observed, in the case of ilmenite, the lower the pH, the higher the activity was that was almost negligible as pH above 6. At an initial pH of 3, both catalysts show a very similar activity. On the contrary, the P25 photoactivity was significantly higher at an initial pH of 6.

These results suggest a scarce photocatalytic activity of ilmenite, despite the high percentage of rutile in its structure. Reactions 6–9 summary the photocatalytic process [4]. According to this scheme, the electron/hole pair generated by irradiating the catalyst with wavelength lower than 400 nm, evolves to produce superoxide radical anions (reaction 7) and hydroxyl radicals (reaction 8), which are responsible of oxidizing organic matter [16].

$$\mathrm{ILM - TiO_2 - FeTiO_3} + h\upsilon^{\lambda<400\mathrm{nm}} \rightarrow e^-_{CB} + h^+_{VB} \quad (6)$$

$$e^-_{CB} + O_2 \rightarrow O_2^{\bullet -} \quad (7)$$

$$h^+_{VB} + H_2O \rightarrow HO^{\bullet} + H^+ \quad (8)$$

$$e^-_{CB} + h^+_{VB} \rightarrow \mathrm{energy}(h\upsilon) \quad (9)$$

In the case of ilmenite, the scheme is modified by the presence of Fe(II) and Fe(III), that act as electrons and/or holes scavengers (reaction 10 and 11) and, therefore, reduce the HO• generation [13].

$$\mathrm{ILM - Fe(III)} + e^-_{CB} \rightarrow \mathrm{ILM - Fe(II)} \quad (10)$$

$$\mathrm{ILM - Fe(II)} + h^+_{VB} \rightarrow \mathrm{ILM - Fe(III)} \quad (11)$$

The low photocatalytic activity of ilmenite may be also attributed to the high Fe/Ti molar ratio that produces an elevated electron/holes pairs recombination (reaction 9) [17,18], leading to a loss of energy and a reduction of the process efficiency [19,20].

3.4. CWPO activity

The presence of iron allows ilmenite for being a feasible catalyst for CWPO processes due to both, the role of iron as active phase and the fact that iron is part of the matrix, which could lead to a highly stable catalyst (7). Besides, as ilmenite is used as received (after a mill treatment), it becomes cheaper than other catalyst [21].

Fig. 5 confirms the catalytic activity of ilmenite in CWPO processes. The generation of HO•radicals occurs as follows:

$$\mathrm{ILM - Fe(II)} + H_2O_2 \rightarrow HO^{\bullet} + OH^- + \mathrm{ILM - Fe(III)} \quad (12)$$

It is noticeable a 3 h induction time at the beginning of the CWPO run, with a scarce variation in phenol and H_2O_2 concentrations. A similar behavior occurs as Fe^{3+} is used as iron source in homogeneous Fenton process, or Fe^{3+}/Υ-Al_2O_3 catalyst [22] in CWPO process. This could indicate that ilmenite, despite the presence of iron in its surface, needs to be activated to promote H_2O_2 decomposition into HO• radicals.

In this sense, the appearance of traces of catechol and hydroquinone in the reaction medium after 3 h reaction time provoked a significant increase into H_2O_2 decomposition and phenol removal. These aromatics byproducts promoted the Fe (III) reduction to Fe (II) [23] increasing the HO• generation rate (reaction 2) and, therefore, the overall oxidation rate. Once these compounds were totally removal, the H_2O_2 decomposition and the oxidation rate decreased significantly.

Phenol was totally removed at the end of the experiments. Nevertheless, H_2O_2 decomposition as well as TOC conversion were not too high (around 50% after 480 min), despites the higher iron concentration in the ilmenite (37%). For the sake of comparison, TOC conversion using alumina or activated carbon iron (4% weight) supported catalysts reached values around 60% and 80%, respectively, after 240 min [22,24]. The amount of iron leached in solution was 2.3 mg L^{-1} (around 1 wt.%).

The evolution of TOC and H_2O_2 through the experiments could provide additional information over the fate of HO• radicals. Fig. 6 shows the evolution of TOC conversion with H_2O_2 conversion. As can be observed, the experimental data assume a linear trend with a slope = 1, which dismisses the occurrence of scavenging reactions. It must be note that the experiments were carried out using the stoichiometric amount of H_2O_2 to mineralize TOC.

3.5. CWPO-Photoassisted activity

The aforementioned results show the limitation of using this solid either as photocatalyst or as catalyst into CWPO process. Nevertheless, in the latest process, the main drawbacks, a high induction time and a lower oxidation rate, could be overcome by irradiating with solar light. Previous work in the literature [25,26] stated the effect of solar light upon the Fe (III)/Fe (II) redox-cycle in ilmenite (reaction 10). Besides, several researches have already combined CWPO with UV and visible light [27,28]. Fig. 7 shows the

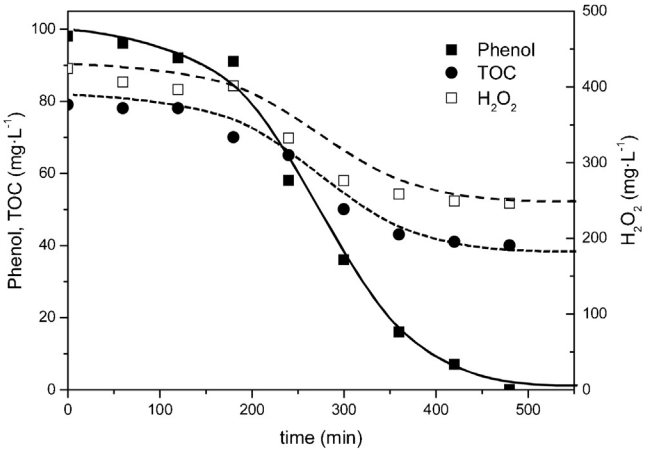

Fig. 5. Phenol, TOC and H_2O_2 evolution during CWPO process with ilmenite (operating conditions: pH = 3; [ilmenite] = 450 mg L^{-1}; [phenol] = 100 mg L^{-1}; [H_2O_2] = 500 mg L^{-1}). Lines show trends.

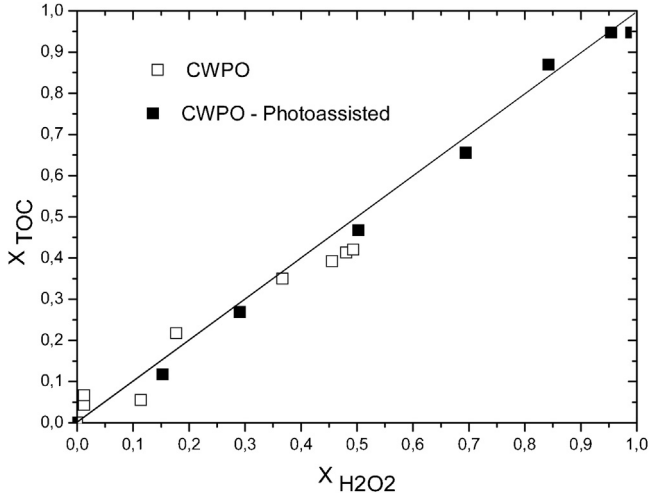

Fig. 6. Comparison of X_{TOC} with X_{H2O2} upon CWPO and CWPO-Photoassisted.

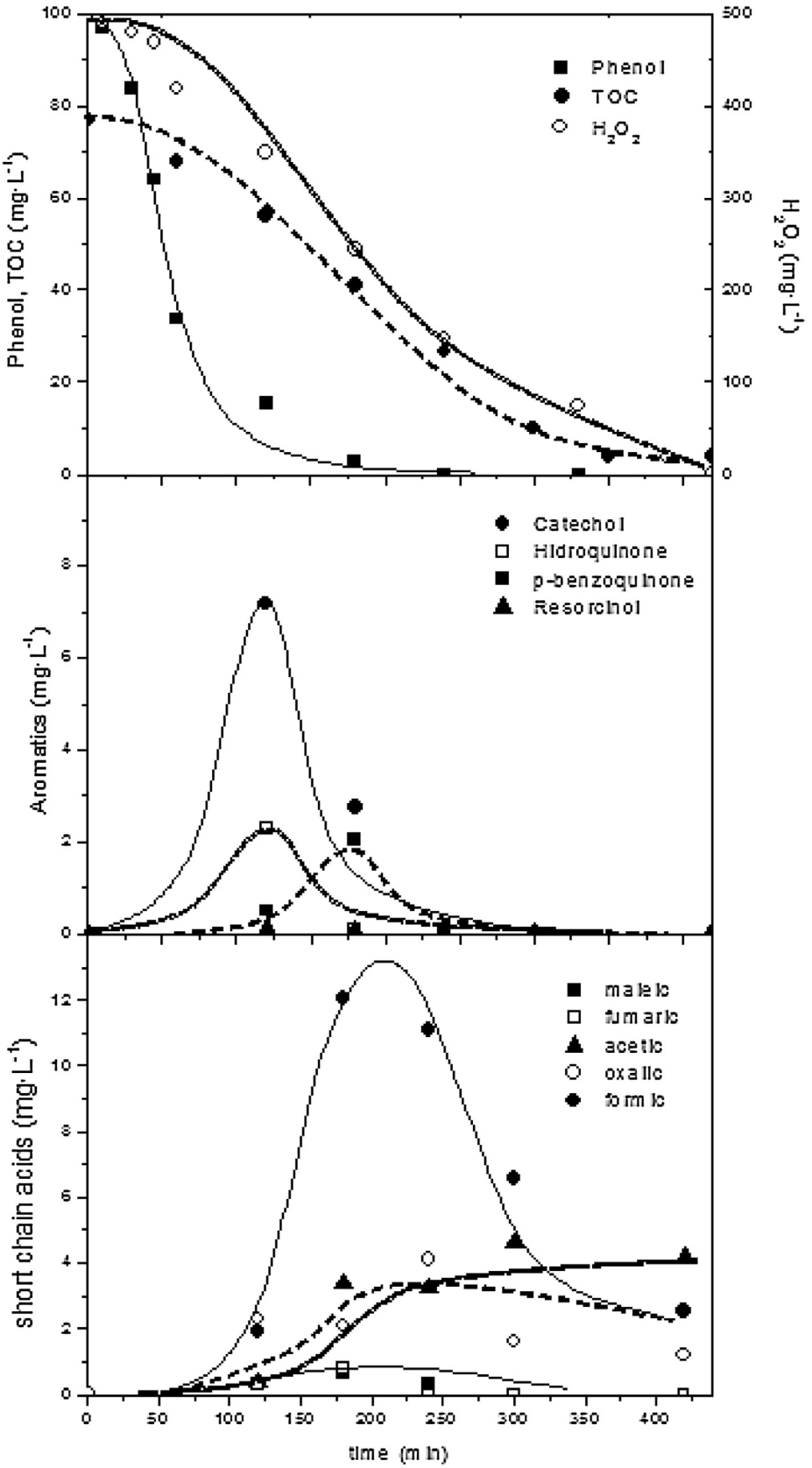

Fig. 7. CWPO-Photoassisted with ilmenite mineral (operating conditions: pH = 3; [Ilmenite] = 450 mg L^{-1}; [phenol] = 100 mg L^{-1}; [H_2O_2] = 500 mg L^{-1}; λ = 300–800 nm; I = 550 W m^{-2}). Lines show trends.

evolution of phenol oxidation by CWPO-Photoassisted process. Blank runs (in absence of catalyst and H_2O_2), photolysis and adsorption experiments were also carried out (data not shown). In all cases, TOC reduction was lower than 10%.

As can be observed, the combined process increases significantly the oxidation rate and the mineralization degree. Thus, total phenol and H_2O_2 conversion as well as 95% TOC depletion were achieved within 480 min reaction time.

These results endorse the synergistic effect of solar light on the catalytic activity of ilmenite that lead to a higher and more efficient production of hydroxyl radicals. Thus, on one hand, solar irradiation have influence upon the Fe (III)/Fe (II) cycle (reaction 10 and 11). On the other hand, the electron/holes pair generated by irradiating ilmenite (reaction 6) react with H_2O_2 giving rise $HO^{\bullet}$ and $HOO^{\bullet}$ radicals, respectively (reaction 14 and 15).

$$e^{-}_{CB} + H_2O_2 \rightarrow HO^{\bullet} + OH^{-} \quad (14)$$

$$h^{+}_{VB} + H_2O_2 \rightarrow HO^{\bullet}_2 + H^{+} \quad (15)$$

Catechol, hydroquinone, benzoquinone and traces of resorcinol were detected in the reaction media. As the reaction progress, these aromatic intermediates were oxidized to short chain acids, mainly maleic, oxalic and formic acid, following a regular oxidation pathway [29]. However, it is noticeable the very low oxalic acid concentration at the end of the reaction that is easily mineralized in presence of solar light, unlike what occurs in dark CWPO, where oxalic acid remains in the reaction media. The amount of leached iron in solutions was very low, lower than 1 mg L^{-1} (0.5 wt.%), confirming the high stability of this solid.

The higher TOC and H_2O_2 conversion led to a higher H_2O_2 yield (η), defined as the amount of TOC removed per unit weight of H_2O_2 fed [30]. The combined process increases this value from 74 (by CWPO alone) to 145. The maximum value of ŋ at complete TOC conversion when using the stoichiometric H_2O_2 dose would be 153 mg TOC/g H_2O_2. H_2O_2 yield, along with the evolution of TOC conversion with H_2O_2 conversion (Fig. 6), discard the occurrence of scavenging reactions. Besides, data shown in Fig. 6 prove the role of solar light as promoter of the ilmenite surface activation, reducing the induction period and increasing H_2O_2 decomposition into $HO^{\bullet}$ radicals.Therefore, ilmenite could be considered a suitable catalyst for CWPO-Photoassisted process due to its two active phases take part in the process achieving complete phenol degradation and 95% of TOC conversion.

To ratify its feasibility as CWPO-Photoassisted catalyst, ilmenite was submitted to five consecutive discontinuous runs. After each run (480 min reaction time), the catalyst was separated by filtration, washed twice with deionized water and dried at 60 °C for 12 h. Table 2 gathers the values of TOC and Fe leached after each run.

As can be observed, the catalytic activity quite slightly decreased after each experiment, being steeper after the third run. This could be caused by a progressive passivation of the ilmenite surface [31]. In terms of stability, the leaching of iron was very low, around 1 wt.% after the first run, decreasing significantly for the next cycles, around 0.3 wt.% each. Besides, TOC conversion was always maintained above 90%, endorsing the suitability of ilmenite as catalyst for CWPO-Photoassisted.

These results confirm the viability of this catalyst in CWPO-Photoassisted process. The presence of iron inside ilmenite structure confers higher stability than the ones obtain by iron supported catalysts [32]. Moreover, ilmenite shows a better activity than the synthesized catalyst which iron in its structure [33].

Table 2
Stability runs at operating conditions of Fig. 7.

Run	$[Fe_{leached}]$ (mg L^{-1})	X_{TOC}
1	0.9	0.95
2	0.3	0.95
3	0.2	0.94
4	0.2	0.93
5	0.2	0.91

4. Conclusions

Ilmenite mineral has shown to be active and highly stable catalyst for CWPO-Photoassisted process. A complete phenol and H_2O_2 conversion and a TOC conversion higher than 95% were reached at pH 3 and 25 °C with 500 mg/L of ilmenite and the stoichiometric amount of H_2O_2. Its activity is a result of the H_2O_2 decomposition into $HO^{\bullet}$ radicals by Fe contained in the ilmenite structure and enhanced by the influence of light upon redox Fe(III)/Fe(II) cycle and the reaction of H_2O_2 with the photogenerated electron/hole pairs which reduce their recombination. The fact that iron is in the catalyst matrix leads to a negligible leaching (0.5 wt.%) and so confirms ilmenite stability.

Acknowledgements

The authors wish to thank the Spanish MINECO for the financial support through the project CTQ2013-41963-R. The Comunidad Autonoma de Madrid is also gratefully acknowledge for the financial support through the project S2013/MAE-2716. P.García-Muñoz acknowledges the UAM for his FPI-UAM 2013 pre-doctoral grant.

References

[1] Y.H. Chen, Synthesis, characterization and dye adsorption of ilmenite nanoparticles, J. Non-Cryst. Solids 357 (2011) 136–139.
[2] T. Fujii, H. Oohashi, T. Tochio, Y. Ito, A. Vlaicu, S. Fukushim, Speculations on anomalous chemical states of Ti ions in $FeTiO_3$ observed by high-resolution X-ray Kβ emission spectra, J. Electron. Spectrosc. Relat. Phenom. 184 (2011) 10–15.
[3] M.E. Zarazúa-Morín, Synthesis, characterization, and catalytic activity of $FeTiO_3/TiO_2$ for photodegradation of organic pollutants with visible light, Res. Chem. Intermed. (2015) , doi:http://dx.doi.org/10.1007/s11164-015-2071-9.
[4] S. Malato, P. Fernández-Ibáñez, M.I. Maldonado, J. Blanco, W. Gernjak, Decontamination and disinfection of water by solar photocatalysis: recent overview and trends, Catal. Today 147 (2009) 1–59.
[5] E. Moctezuma, B. Zermeño, E. Zarazua, L. Torres-Martínez, R. García, Photocatalytic degradation of phenol with Fe-titania catalysts, Top. Catal. 54 (2011) 496–503.
[6] A. Teel, D. Finn, J. Schmidt, L. Cutler, R. Watts, Rates of trace mineral-catalyzed decomposition of hydrogen peroxide, J. Environ. Eng. 133 (2007) 853–858.
[7] J.A. Zazo, J. Bedia, C.M. Fierro, G. Pliego, J.A. Casas, J.J. Rodriguez, Highly stable Fe on activated carbon catalysts for CWPO upon FeCl3 activation of lignin from black liquors, Catal. Today 187 (2012) 115–121.
[8] E. Brillas, E. Mur, R. Sauleda, L. Sànchez, J. Peral, X. Domènech, et al., Aniline mineralization by AOP's: anodic oxidation, photocatalysis, electro-Fenton and photoelectro-Fenton processes, Appl. Catal. B Environ. 16 (1998) 31–42.
[9] E.B. Sandell, Colorimetric determination of traces of metals, J. Phys. Chem. 49 (1945) 263–264.
[10] A.A. Baba, S. Swaroopa, F.A. Ghoshmk Adekola, Mineralogical characterization and leaching behaviour of Nigerian ilmenite ore, Trans. Nonferrous Met. Soc. China 23 (2013) 2743–2750.
[11] T. Yamashita, P. Hayes, Analysis of XPS spectra of Fe^{2+} and Fe^{3+} ions in oxide materials, Appl. Surf. Sci. 254 (2008) 2441–2449.
[12] A.T. Raghavender, H. Hoa, N. ong, L. Joon, K. ee, M. Jung, Z. Skoko, M. Vasilevskiy, et al., Nano-ilmenite $FeTiO_3$: synthesis and characterization, J. Magn. Magn. Mater. 331 (2013) 129–132.
[13] M. Schoonen, X. aa, Y. u, D.R. Strongin, An introduction to geocatalysis, J. Geochem. Explor. 62 (1998) 201–215.
[14] Y.R. Smith, K. Joseph Antony Raj, V. Subramanian, B. Viswanathan, Sulfated Fe2O3–TiO2 synthesized from ilmenite ore: a visible light active photocatalyst, Colloids Surf. 367 (2010) 140–147.
[15] Y. Yalçın, M. Kılıç, Z. Çınar, Fe^{3+}-doped TiO_2: a combined experimental and computational approach to the evaluation of visible light activity, Appl. Catal. B Environ. 99 (2010) 469–477.

[16] E.S. Elmolla, M. Chaudhuri, Photocatalytic degradation of amoxicillin, ampicillin and cloxacillin antibiotics in aqueous solution using UV/TiO2 and UV/H_2O_2/TiO_2 photocatalysis, Desalination 252 (2010) 46–52.
[17] Q.D. Truong, J. Liu, C. Chung, Y. Ling, Photocatalytic reduction of CO_2 on $FeTiO_3$/TiO_2 photocatalyst, Catal. Commun. 19 (2012) 85–89.
[18] M. Qamar, B. Merzougui, D. Anjum, A.S. Hakeem, Z.H. Yamani, D. Bahnemann, Synthesis and photocatalytic activity of mesoporous nanocrystalline Fe-doped titanium dioxide, Catal. Today 230 (2014) 158–165.
[19] H. Mĕšťánková, G. Mailhot, J. Jirkovský, J. Krýsa, M. Bolte, Mechanistic approach of the combined (iron–TiO_2) photocatalytic system for the degradation of pollutants in aqueous solution: an attempt of rationalisation, Appl. Catal. B Environ. 57 (2005) 257–265.
[20] J. Herrmann, Fundamentals and misconceptions in photocatalysis, J. Photochem. Photobiol. A 216 (2010) 85–93.
[21] M. Hartmann, S. Kullmann, H. Keller, Wastewater treatment with heterogeneous Fenton-type catalysts based on porous materials, J. Mater. Chem. (2010) , doi:http://dx.doi.org/10.1039/c0jm00577k.
[22] P. Bautista, A.F. Mohedano, J.A. Casas, J.A. Zazo, J.J. Rodríguez, Highly stable Fe/γ-Al2O3 catalyst for catalytic wet peroxide oxidation, J. Chem. Technol. Biotechnol. 86 (2011) 497–504.
[23] R. Chen, J. Pignatello, Role of quinone intermediates as electron shuttles in Fenton and photoassisted Fenton oxidations of aromatic compounds, Environ. Sci. Technol. 31 (1997) 2399–2406.
[24] J.A. Zazo, J.A. Casas, A.F. Mohedano, J.J. Rodríguez, Catalytic wet peroxide oxidation of phenol with a Fe/active carbon catalyst, Appl. Catal., B: Environ. 65 (2006) 261–268.
[25] Y.R. Wang, W. Chu, Photo-assisted degradation of 2,4,5-trichlorophenoxyacetic acid by Fe (II)-catalysed activation of oxone process: the role of UV irradiation, reaction mechanism and mineralization, Appl. Catal. B Environ. 123–124 (2012) 151–161.
[26] H. Fallmann, T. Krutzler, R. Bauer, S. Malato, J. Blanco, Applicability of the photo-Fenton method for treating water containing pesticides, Catal. Today 54 (1999) 309–319.
[27] H. Bel, H. adjltaief, C. Da, P. osta, P. Beaunier, M.E. Gálvez, Z. Ben, M. ina, Fe-clay-plate as a heterogeneous catalyst in photo-Fenton oxidation of phenol as probe molecule for water treatment, Appl. Clay Sci. 91-92 (2014) 46–54.
[28] M. Minella, G. Marchetti, L. De, E. aurentiis, M. Malandrino, V. Maurino, C. Minero, et al., Photo-Fenton oxidation of phenol with magnetite as iron source, Appl. Catal. B Environ. 154–155 (2014) 102–109.
[29] J.A. Zazo, Chemical pathway and kinetics of phenol oxidation by Fenton's reagent, Environ. Sci. Technol. 39 (2005) 9295–9302.
[30] J.A. Zazo, J.A. Casas, A.F. Mohedano, J.J. Rodriguez, Semicontinuous Fenton oxidation of phenol in aqueous solution. A kinetic study, Water Res. 43 (2009) 4063–4069.
[31] Y. Segura, F. Martínez, J.A. Melero, J.L.G. Fierro, Zero valent iron (ZVI) mediated Fenton degradation of industrial wastewater: treatment performance and characterization of final composites, Chem. Eng. J. 269 (2015) 298–305.
[32] M. Munoz, Z.M. de Pedro, N. Menendez, J.A. Casas, J.J. Rodriguez, A ferromagnetic γ-alumina-supported iron catalyst for CWPO. Application to chlorophenols, Appl. Catal. B Environ. 136–137 (2013) 218–224.
[33] R.S. Ribeiro, A.M.T. Silva, J.L. Figueiredo, J.L. Faria, H.T. Gomes, Removal of 2-nitrophenol by catalytic wet peroxide oxidation using carbon materials with different morphological and chemical properties, Appl. Catal. B Environ. 140–141 (2013) 356–362.